Contemporary Mathematics
http://ojs.wiserpub.com/index.php/CM/

UNIVERSAL WISER PUBLISHER

Research Article

# An Application of the Melnikov Method to a Piecewise Oscillator

**Oltiana Gjata, Fabio Zanolin*** 

Department of Mathematics, Computer Science and Physics, University of Udine, Via delle Scienze 206, 33100 Udine, Italy
E-mail: fabio.zanolin@uniud.it

**Received:** 14 November 2022; **Revised:** 29 March 2023; **Accepted:** 12 April 2023

**Abstract:** In this paper we present a new application of the Melnikov method to a class of periodically perturbed Duffing equations where the nonlinearity is non-smooth as otherwise required in the classical applications. Extensions of the Melnikov method to these situations is a topic with growing interests from the researchers in the past decade. Our model, motivated by the study of mechanical vibrations for systems with "stops", considers a case of a nonlinear equation with piecewise linear components. This allows us to provide a precise analytical representation of the homoclinic orbit for the associated autonomous planar system and thus obtain simply computable conditions for the zeros of the associated Melnikov function.

***Keywords*:** Duffing equation, homoclinic trajectory, non-smooth systems, chaotic dynamics, Melnikov method

**MSC:** 34C25, 34B18, 34C35

## 1. Introduction

The aim of this paper is to provide a new application of the Melnikov method to a class of periodically perturbed Duffing equations which are characterized by the presence of a piecewise smooth vector field.

The Melnikov method [1], following the pioneering work of Poincaré, considers a $\varepsilon$-$T$-periodic perturbation $\varepsilon Y(t, z)$ of an autonomous planar system $\dot{z} = X_0(z)$, possessing a homoclinic trajectory $\gamma_0(t)$ at the origin, which is assumed to be a hyperbolic saddle point. Under very natural assumptions, it is proved that, for $\varepsilon \neq 0$ sufficiently small, the Poincaré map $\Phi_\varepsilon^{t_0}$ at the time $t_0$, associated with the system

$$\dot{z} = X_0(z) + \varepsilon Y(t, z),$$

has a (unique) hyperbolic saddle point $P_\varepsilon^{t_0}$ near the origin (corresponding to a unique hyperbolic periodic orbit $\gamma_\varepsilon \sim 0$) with its local stable $W^s(P_\varepsilon^{t_0})$ and unstable $W^u(P_\varepsilon^{t_0})$ manifolds close to those of the unperturbed system. As explained in [2, Section 4.5], in order to study the separation of the two mmanifolds, an auxiliary integral function $M(\cdot)$ is introduced, depending on $\gamma_0(t)$ and the perturbed term, in the form of


DOI: https://doi.org/10.37256/cm.4220232160

$$M(\alpha) := \int_{-\infty}^{+\infty} X_0(\gamma_0(t-\alpha)) \wedge Y(t, \gamma_0(t-\alpha))dt.$$

It holds that the existence of a simple zero $\alpha_0$ for the Melnikov function $M(\alpha)$ implies the transversal intersections of $W^s(P_\varepsilon^{\alpha_0})$ and $W^u(P_\varepsilon^{\alpha_0})$ for $\varepsilon \neq 0$ and sufficiently small. As a consequence, the Smale-Birkhoff homoclinic theorem [3, 4] (see also [2, Theorem 5.3.5], [5, Theorem 3.7]), implies that some iterate of the Poincaré map $\Phi_\varepsilon^{\alpha_0}$ has a hyperbolic invariant set, namely a *Smale mhorseshoe*, where it is conjugate to the Bernoulli shift automorphism on two (or more) symbols.

The Melnikov method is a powerful tool to prove rigorously the presence of complex dynamics in periodically perturbed systems. There are, however, some difficulties in its applications to planar (or higher-dimensional) dynamical systems arising from actual models. The first problem may arise when an explicit form of the homoclinic orbit $\gamma_0(t)$ is unknown. For some equations, this difficulty can be overcome by exploiting some symmetries on $\gamma_0(t)$ and the perturbed terms as in [6], or through a deeper analysis on the function $M(\alpha)$ as in [7]. The second possible problem comes from the hypotheses of regularity on the vector fields which are required for the applicability of the theorems. In [1], the maps are assumed to be analytic, while in [8] the class $C^\infty$ is required. Apparently, the minimal regularity hypotheses are those in the treatment of the topic by Guckenheimer and Holmes [2], where the vector fields are assumed to be "sufficiently smooth" of class $C^r$ with $r \geq 2$. However, even assuming the minimal regularity conditions, there are several interesting models (for instance, coming from mechanical systems [9]) where the "classical theory" cannot be applied for lack of regularity.

In last decades, a great deal of interest has been devoted to the extension of some classical methods of dynamical systems, like KAM theory, to nonsmooth differential systems (see [10, 11]). Shaw and Holmes in [12] and Ortega in [11] exhibit specific mechanical models which are modelled by piecewise smooth restoring forces. Concerning the Melnikov method, in the recent years several interesting extensions have been achieved by different authors. The articles [13-26] and the references therein (just to mention a few main recent contributions in this area of research), show the great deal of interest in this topic both from the theoretical and the applied point of view. Most of the achieved results are general enough to cover the case of piecewise smooth differential systems which present a manifold of discontinuity. The application we consider in the present article deals with a simpler situation, namely the case of a Lipschitz continuous planar vector field which is smooth (indeed of class $C^\infty$) except for a single vertical line which intersects transversally the homoclinic orbit. More in detail, we reconsider, in the light of the Melnikov method, a model previously studied by Pokrovskii, Rasskazov and Visetti in [27] dealing with the periodically perturbed Duffing-type equation

$$\ddot{x} + \varepsilon c\dot{x} = \varepsilon p(\omega t) + s(x), \tag{1}$$

where $s(x)$ is a truncated signum function, that is it coincides with $x/|x|$ for $|x| \geq d > 0$ and is linear for $|x| \leq d$. As shown in [9, 11] and also recalled in [27], equations of this form arise in the engineering literature as models of oscillators with *stops*. Also Holmes and Moon [28, 29] showed how to produce a large variery of Duffing-type equations with different restoring forces, by combining mechanical and magnetic effects in buckled magnetoelastic oscillators. For our application we will employ a theorem by Li, Gong, Zhang and Hao in [23] which is well suited to our model.

In [27], the case $c = 0$, $\varepsilon = 1$, and $p(t) = \sin(t)$ was consider for the special value of $\omega = \sqrt{2}$. The result in [27] is topological and global in nature and does not require the smallness of the forcing term $p(t)$. The "chaotic dynamics" obtained in [27] is that of a *topological horseshoe* [30] (or also [31-33]), which provides a semi-conjugation with the Bernoulli shift (actually, a weaker form of *semi-conjugation* is obtained in [27, Definition 2.1]). On the other hand, using the Melnikov approach, we are able to deal with a wide range of frequencies $\omega$ (see Lemma 3.1 and Figure 1) and to prove the existence of a stronger form of chaotic dynamics, that is the conjugation with the Bernoulli shift due to the presence of a Smale horseshoe.

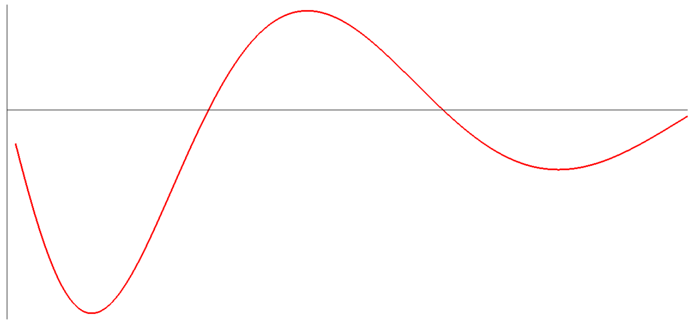

**Figure 1.** Approximate graph associated with the function $N(\omega)$ for $\omega \in [0.1, 8]$. Using Maple software, we find that the first zero $\omega_1$ of $N(\omega)$ should belong to the interval [2.367, 2.368] and the second zero, $\omega_2$ of $N(\omega)$ should belong to the interval [5.122, 5.123]

The plan of the paper is the following. In Section 2, following [2], we recall, for the reader's convenience, some basic facts on Melnikov method for the periodically perturbed scalar Duffing equation

$$\ddot{x} + c\dot{x} + g(t, x) = 0,$$

considered, in the phase-plane, as a perturbation of the autonomous system

$$\dot{x} = y,\ \dot{y} = -g(x) = 0.$$

For this system we will assume the existence of a hyperbolic saddle point at the origin with a homoclinic trajectory. In Section 3 we apply the Melnikov theory, in the variant for non-smooth systems described in [22, 23, 25], to equation (1). Finally, Section 4 provides some numerical examples illustrating the chaotic nature of the solutions whose existence has been proved analytically in Section 3.

## 2. A brief introduction to the Duffing equation

One of the simplest but more widely studied examples of a planar conservative systems is given by the two-dimensional system

$$\begin{cases} \dot{x} = y \\ \dot{y} = -g(x) \end{cases} \tag{2}$$

which corresponds to the scalar equation

$$\ddot{x} + g(x) = 0 \tag{3}$$

in the phase-plane.

Throughout the section we will suppose that $g : J \to \mathbb{R}$ is a locally Lipschitz continuous function defined on an open interval $J \subseteq \mathbb{R}$ where $g$ vanishes at least in a point. Without loss of generality (using, if necessary, a simple change of variables) we can suppose that $0 \in J$ and $g(0) = 0$, so that the origin is an equilibrium point of (2). In general, a point $P = (x_0, y_0)$ is an equilibrium point for (2) if and only if $y_0 = 0$ and $g(x_0) = 0$.

System (2) is a planar Hamiltonian system with associated Hamiltonian (energy function)

$$H(x,y)=\frac{1}{2}y^2+G(x),\ G(x)=\int_0^x g(s)ds.$$

As a consequence, the orbits of (2) are contained in the level sets of $H$. In fact, if $(x(t), y(t))$ is any solution of (2) then $(x(t), y(t)) \in \Gamma^c$ for all $t$, where

$$\Gamma^c := \{(x,y)\in\mathbb{R}^2 : H(x,y)=c\},\ \text{for } c = H(x(0), y(0)).$$

Equation (3) is the *autonomous* Duffing equation, named after Georg Duffing (1861-1944). A large literature, still growing up, has been devoted to the investigation of the perturbations of (3) by periodic forcing terms, as well as by damping terms, leading to

$$\ddot{x}+g(t,x)=0 \tag{4}$$

and to

$$\ddot{x}+c\dot{x}+g(t,x)=0, \tag{5}$$

respectively. Usually, in (4) and (5) the nonlinear restoring force $g : \mathbb{R} \times J \to \mathbb{R}$ is a continuous function, locally Lipschitzian in the $x$-variable and periodic in the $t$-variable of a fixed period $T > 0$. The domain $J$ for the $x$-variable in an open interval of the real line. The most common case is given by $J = \mathbb{R}$, however research has been devoted also to the case when $J \neq \mathbb{R}$, in order to describe some physical models where the points at the boundary of $J$ represent possible singularities of the vector field.

Classical results on the Duffing equation can be found in the books of J. K. Hale [34] and Guckenheimer and Holmes [2]. In [35] the study of harmonic and subharmonic solutions for (4) was performed in the case $J = \mathbb{R}$, while in [36, 37] the cases $J = [0, +\infty]$ and $J = [a, b]$ where considered as well.

Concerning the presence of chaotic-like solutions in [2, Section 4.5] the Melnikov method is applied to the perturbed equation

$$\ddot{x}+\varepsilon c\dot{x}+g(x)=\varepsilon p(\omega t), \tag{6}$$

where $c, \varepsilon, \omega > 0$ and $p(\cdot)$ is a non-constant periodic forcing term. According to [2], the functions $g(x)$ and $p(t)$ should be sufficiently smooth (of class $C^r$ with $r \geq 2$).

The main assumption in [2] is the presence of a homoclinic solution $\gamma_0(t) = (q_0(t), v_0(t))$ at the origin for the autonomous system (2). Associated with $\gamma(t)$, the Melnikov function

$$M(\alpha) := \int_{-\infty}^{+\infty}\left(v_0(t)p(\omega(t+\alpha)) - cv_0(t)^2\right)dt$$

is introduced. Melnikov's theory (cf. [2, Theorem 4.5.3]) guarantees that, if $M(\alpha)$ has a simple zero for some $\alpha = \alpha_0$, then, for $\varepsilon > 0$ sufficiently small, there exists a hyperbolic equilibrium point $P_\varepsilon^{\alpha_0}$ near the origin for system

$$\begin{cases}\dot{x}=y\\ \dot{y}=-g(x)-\varepsilon p(\omega t)-\varepsilon cy\end{cases} \tag{7}$$

such that its stable and unstable manifolds $W^s(P_\varepsilon^{\alpha_0})$ and $W^u(P_\varepsilon^{\alpha_0})$ intersect transversely. This property, in turn, via the Smale-Birkhoff theorem, implies that some $N$-th iterate of the Poincaré map $\Phi_\varepsilon$ associated with system (7), has a Smale horseshoe and therefore it has an invariant set where it is conjugate to the Bernoulli shift on a set of symbols. As a consequence, $\Phi_\varepsilon^N$ presents chaotic dynamics in the sense of Devaney. Further relevant results in this directions can be found in [38] for the equation

$$\ddot{x} + \lambda a(t) g(x) = 0$$

and in [7] for

$$\ddot{x} + g(x) = \varepsilon p(t).$$

The Melnikov method, although very powerful and relevant from the point of view of the applications is typically applied in situations where the unperturbed Duffing system (2) possesses homoclinic or heteroclinic solutions. Moreover, the analysis of the Melnikov function $M(\alpha)$ or its variants can be extremely difficult when an explicit analytic form of the homoclinic solution $\gamma(t)$ is unknown. Finally, the result allows to make conclusions for small perturbations, namely for $\varepsilon > 0$ sufficiently small.

A classical application of the Melnikov method to the periodically perturbed Duffing equation (6) deals with the case

$$g(x) = -x + x^3. \tag{8}$$

This example is motivated by a concrete mechanical vibrational model studied in the pioneering work [39] end exposed also in [2]. In this situation, for the associated autonomous system (3), the origin is a saddle point and the energy level line $H(x, y) = 0$, that is

$$\frac{1}{2}y^2 - \frac{1}{2}x^2 + \frac{1}{4}x^4 = 0$$

is composed by two homoclinic orbits

$$\Gamma_+^0 := \{(x, y) : x > 0, H(x, y) = 0\}, \ \Gamma_-^0 := \{(x, y) : x < 0, H(x, y) = 0\}$$

and the origin. Each of the orbits $\Gamma_\pm^0$ is the locus of a homoclinic solution $\gamma_0^\pm(t) = (q_0^\pm(t), v_0^\pm(t))$, for which an explicit analytical expression is known, namely:

$$q_0^+(t) = \sqrt{2}\operatorname{sech} t, \ v_0^+(t) = -\sqrt{2}(\operatorname{sech} t)(\tanh t)$$

and $\gamma_0^-(t) = -\gamma_0^+(t)$.

Then, in case of (7) with $g(x)$ as in (8), we can compute the Melnikov function for $\gamma_0^+(t)$ as follows (with $v_0 = v_0^+$).

$$M(\alpha) = \int_{-\infty}^{+\infty} \left( v_0(t) p(\omega(t+\alpha)) - c v_0(t)^2 \right) dt$$

$$= -\sqrt{2}\int_{-\infty}^{+\infty} (\operatorname{sech} t)(\tanh t) p(\omega(t+\alpha)) dt - 2c\int_{-\infty}^{+\infty} (\operatorname{sech}^2 t)(\tanh^2 t) dt.$$

Using the fact that $\int_{-\infty}^{+\infty} (\operatorname{sech}^2 t)(\tanh^2 t) dt = \frac{2}{3}$, we obtain the explicit formula

$$M(\alpha) = -\frac{4}{3}c - \sqrt{2}\int_{-\infty}^{+\infty} (\operatorname{sech} t)(\tanh t)\, p(\omega(t+\alpha))\,dt.$$

This latter expression can be evaluated whenever a specific analytical expression of $p(t)$ is known. For instance, following [2], for

$$p(t) := E\cos(\omega t),$$

the following form of $M(\alpha)$ is obtained.

$$M(\alpha) = -\frac{4}{3}c - \sqrt{2}E\int_{-\infty}^{+\infty} (\operatorname{sech} t)(\tanh t)\cos(\omega(t+\alpha))\,dt$$

$$= -\frac{4}{3}c - \sqrt{2}E\cos(\omega\alpha)\int_{-\infty}^{+\infty} (\operatorname{sech} t)(\tanh t)\cos(\omega t)\,dt$$

$$+\sqrt{2}E\sin(\omega\alpha)\int_{-\infty}^{+\infty} (\operatorname{sech} t)(\tanh t)\sin(\omega t)\,dt.$$

Since the function $t \mapsto (\operatorname{sech} t)(\tanh t)$ is odd (see Figure 2), the first of the above integrals in $M(\alpha)$ vanishes.

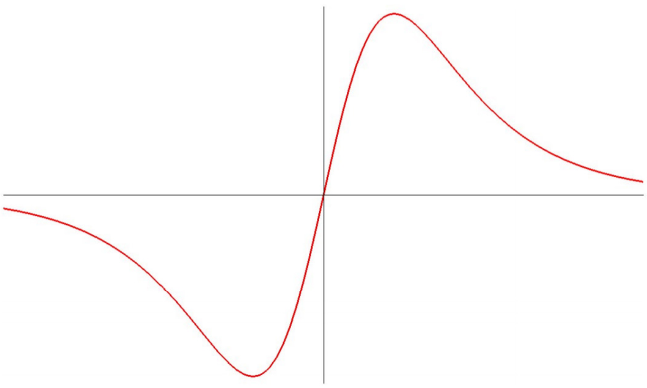

**Figure 2.** Graph associated with the function $t \mapsto (\operatorname{sech} t)(\tanh t)$

Concerning the second integral, we observe that the function $t \mapsto (\operatorname{sech} t)(\tanh t)\sin(\omega t)$ is even, so that

$$\int_{-\infty}^{+\infty} (\operatorname{sech} t)(\tanh t)\sin(\omega t)\,dt = 2\int_{0}^{+\infty} (\operatorname{sech} t)(\tanh t)\sin(\omega t)\,dt := K(\omega).$$

The analytical expression of $K(\omega)$ can be found using the method of the residues (cf. [2]) and is given by

$$K(\omega) = \pi\omega\operatorname{sech}\left(\frac{\pi\omega}{2}\right).$$

In conclusion, for (7) with $g(x)$ as in (8) and in the special case of $p(t) = E\cos(t)$, we obtain

$$M(\alpha) = \sqrt{2}EK(\omega)\sin(\omega\alpha) - \frac{4}{3}c.$$

This function has simple zeros in the variable $\alpha$ (for $c$ not too large) and therefore the Melnikov method guarantees the presence of chaotic dynamics for a $N$-th iterate of the Poincaré map associated with system (7) for $\varepsilon > 0$ sufficiently small, provided that $E > \dfrac{4c}{3\sqrt{2}K(\omega)}$.

As one can see from this example taken from [2], the Melnikov method in principle can be applied to a wide class of equations; on the other hand, it may be very difficult to prove the result about the existence of simple zeros for the function $M(\alpha)$ without knowing the specific analytical expression of the homocinic solution. In [7], Battelli and Palmer found a general result for the Duffing equation

$$\ddot{x} + a^2 g(x) = p(t), \tag{9}$$

where $p(t)$ is a $T$-periodic and both $g(x)$ and $p(t)$ are sufficiently smooth (at least of class $C^{r+3}$ for $r \geq 5$). Assuming the existence of homoclinic or heteroclinic points $z^{\pm}$ with

$$g(z^{\pm}) = 0,\ g'(z^{\pm}) < 0$$

for the autonomous equation

$$\ddot{x} + g(x) = 0,$$

the Authors in [7] proved the existence of transversal intersection (as in Melnikov theorem) for the Poincaré map associated with (9), provided that $a > 0$ is sufficiently large and one of the following conditions holds:

- $z^+ \neq z^-$ and there exists $t_0$ such that $p(t_0) = 0 \neq p'(t_0)$; The caseof heteroclinic points;
- $z^+ = z^-$ and there exists $t_0$ such that $p'(t_0) = 0 \neq p''(t_0)$ The case of homoclinic points.

The advantage of this result with respect to the classical Melnikov formulation (as presented in [2]) depends on the fact that an explicit analytic expression for the homoclinic/heteroclinic solutions is not needed. There are still, however, some assumptions on the forcing term which require simple zeros or simple zeros for the derivative.

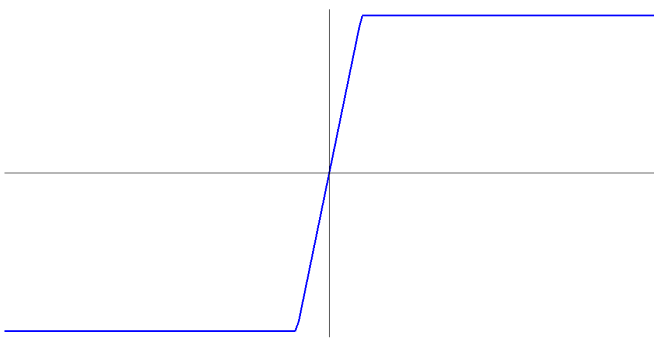

**Figure 3.** Graph associated with the function $s(x)$

## 3. An application of the Melnikov method

In this section, we show a new application of the Melnikov method, described in the preceding section, to a second-order Duffing equation previously considered in [27]. More precisely, in [27] the Authors consider the piecewise linear oscillator

$$\ddot{x} + x = \sin(\sqrt{2}t) + s(x),$$

where

$$s(x) := \begin{cases} -1, & \text{for } x \leq -\dfrac{1}{5} \\ 5x, & \text{for } -\dfrac{1}{5} \leq x \leq +\dfrac{1}{5} \\ 1, & \text{for } x \geq \dfrac{1}{5} \end{cases}$$

(see Figure 3).

The proofs in [27] apply a method based on topological degree theory, for which some geometric conditions must be satisfied. In order to check these geometric assumptions, computer assisted proof is used to verify the inequalities required in the application of the topological techniques. Here we propose a different approach based on recent variants of the Melnikov method to non-smooth (possibly discontinuous) systems which have been developed in [13, 14]. In particular, we find that the results in [22, 23] fits well with our situation, where the manifold separating the regions of smoothness is just a vertical line which is transversal to the homoclinic orbit (see Figure 4). A similar geometric configuration (for a different nonlinearity) has been also discussed in [25].

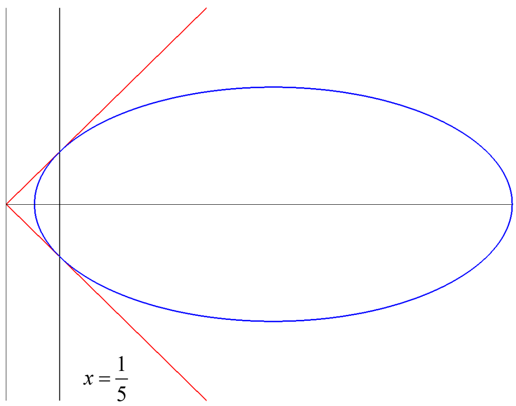


**Figure 4.** Graphs associated with the lines $y = \pm 2x$ and with the circumference $\mathcal{C}$. All these lines/curves intersect transversally the line $x = \frac{1}{5}$ where the vector field is not smooth. In the picture, for typographical reasons, the aspect-ratio has been modified, using a different scale for the $x$ and the $y$ axes, as in Figure 7

We study a periodic perturbation of the autonomous Duffing equation

$$\ddot{x} + \psi(x) = 0, \tag{10}$$

where

$$\psi(x) := x - s(x),$$

for $s(x)$ the piecewise linear function defined as above, so that

$$\psi(x) := \begin{cases} x+1, & \text{for } x \leq -\dfrac{1}{5} \\ -4x, & \text{for } -\dfrac{1}{5} \leq x \leq +\dfrac{1}{5} \\ x-1, & \text{for } x \geq \dfrac{1}{5} \end{cases} \tag{11}$$

(see Figure 5).

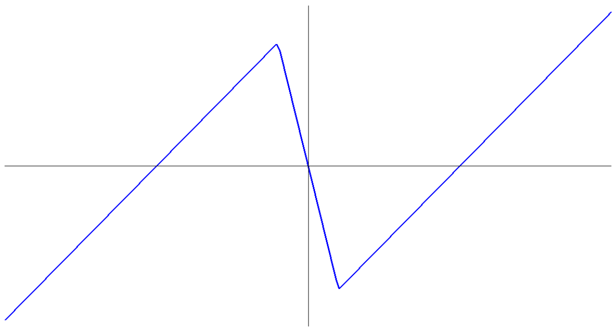

**Figure 5.** Graph associated with the function $\psi(x)$

We will also discuss the perturbations due to the introduction of a small damping term (see equation (11) below).
By definition, the function $\psi$ has exactly three zeros, namely, $-1$, $0$, $1$.
Passing to the phase-plane, equation (10) writes as the autonomous Hamiltonian system

$$\begin{cases} \dot{x} = y \\ \dot{y} = -\psi(x) \end{cases} \tag{12}$$

with Hamiltonian (energy function)

$$H(x, y) = \frac{1}{2}y^2 + \Psi(x), \ \ \Psi(x) = \int_0^x \psi(s)ds.$$

An explicit computation shows that

$$\Psi(x) := \begin{cases} \dfrac{1}{2}x^2 + x + \dfrac{1}{10}, & \text{for } x \le -\dfrac{1}{5} \\ -2x^2, & \text{for } -\dfrac{1}{5} \le x \le +\dfrac{1}{5} \\ \dfrac{1}{2}x^2 - x + \dfrac{1}{10}, & \text{for } x \ge \dfrac{1}{5} \end{cases}$$

(see Figure 6).

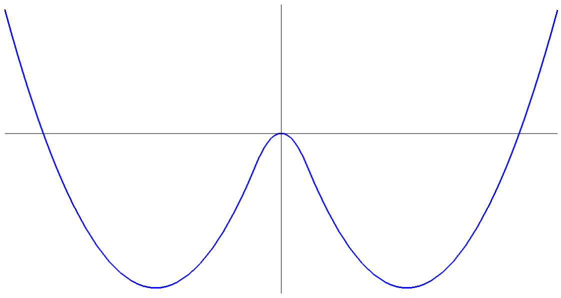

**Figure 6.** Graph associated with the function $\Psi(x)$

The phase-portrait associated with system (12) shows that there are three equilibrium points $-P = (-1, 0)$, $0 = (0, 0)$ and $P = (1, 0)$. The points $-P$ and $P$ are two centers surrounded by two orbits $\mathcal{O}^-$ and $\mathcal{O}^+$ (respectively) which are homoclinic trajectories to the origin, which is a saddle point.

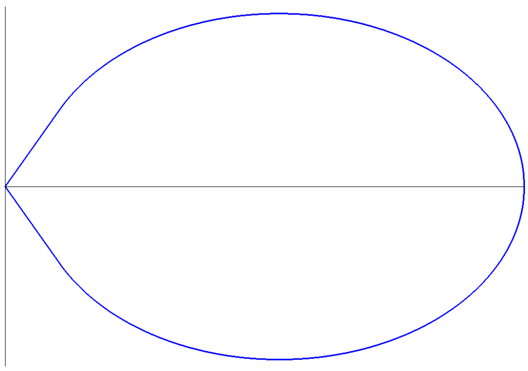

**Figure 7.** Graphs associated with the functions $y = \pm\sqrt{-2\Psi(x)}$ which define the homoclinic orbit $\mathcal{O}^+$. In the picture, for typographical reasons, the aspect-ratio has been modified, using a different scale for the $x$ and the $y$ axes. Actually the part of the homoclinic with $x \ge 1/5$ is a circumference with center at (1, 0)

In the sequel, we focus our attention on the homoclinic orbit contained in the right-half plane, which is described as the zero-level line of $\Psi$ with $x > 0$, namely

$$\mathcal{O}^+ = \{(x, y) : x > 0, H(x, y) = 0\}.$$

The line $\mathcal{O}^+$ intersects the positive $x$-axis at the point

$$Q = \left(1 + \frac{2}{\sqrt{5}}, 0\right) \tag{13}$$

and can be expressed as the union of the graphs of the functions

$$y = \sqrt{-2\Psi(x)},\ y = -\sqrt{-2\Psi(x)}$$

(see Figure 7).

By symmetry, we restrict for a moment our analysis to the upper graph, that is the part of the homoclinic orbit contained in the first quadrant. A direct computation shows that the homoclinic is described by

$$y = 2x, \text{ for } 0 < x \le \frac{1}{5} \tag{14}$$

and

$$y = \sqrt{2x - x^2 - \frac{1}{5}}, \text{ for } \frac{1}{5} \le x \le 1 + \frac{2}{\sqrt{5}}. \tag{15}$$

Similarly, for $y \le 0$ we have

$$y = -2x, \text{ for } 0 < x \le \frac{1}{5} \tag{16}$$

and

$$y = -\sqrt{2x - x^2 - \frac{1}{5}}, \text{ for } \frac{1}{5} \le x \le 1 + \frac{2}{\sqrt{5}}. \tag{17}$$

In this manner, we see that the homoclinic orbit $\mathcal{O}^+$ can be described as follows:

• The local unstable manifold of the origin, contained in the half-line $y = 2x$, for $x > 0$;

• The circumference $\mathcal{C}$ of equation

$$5x^2 + 5y^2 - 10x + 1 = 5((x-1)^2 + y^2) - 4 = 0$$

with center at (1, 0) and radius $2/\sqrt{5}$ ;

• The local stable manifold of the origin, contained in the half-line $y = -2x$.

Observe that the lines $y = \pm 2x$ and the circumference $\mathcal{C}$ intersect transversally the vertical line $x = \frac{1}{5}$, which is the manifold where the planar vector field $(y, -\psi(x))$ is not smooth (see Figure 4). In this manner we can enter in the setting of the Melnikov theory for non-smooth systems developed in [13, 22, 23].

As a next step, we define analytically the Melnikov function. To this end, we need to find an explicit parametric expression of the homoclinic orbit $\mathcal{O}^+$ by means of a solution of the autonomous Duffing equation (12). This task is solved by considering separately the differential equations

$$\ddot{x} - 4x = 0, \, 0 < x(t) \leq \frac{1}{5} \tag{18}$$

and

$$\ddot{x} + x - 1 = 0, \quad \frac{1}{5} \leq x(t) \leq 1 + \frac{2}{\sqrt{5}}. \tag{19}$$

The first equation corresponds to the system

$$\begin{cases} \dot{x} = y \\ \dot{y} = 4x \end{cases} \quad \text{in the strip } \left[0, \frac{1}{5}\right] \times \mathbb{R}, \tag{20}$$

while, for the second one, we have

$$\begin{cases} \dot{x} = y \\ \dot{y} = 1 - x \end{cases} \quad \text{in the strip } \left[\frac{1}{5}, 1 + \frac{2}{\sqrt{5}}\right] \times \mathbb{R}, \tag{21}$$

as equivalent system.

In order to find the homoclinic solution, we have to find the solution of system (21) passing through the point $Q$ defined in (13) and to glue it with the solutions corresponding to the local unstable and stable manifolds of the origin, which are obtained, solving (20).

*The local unstable manifold at the origin*. We solve the system (20), looking for solutions $(x(t), y(t))$ with $x(t) > 0$, $y(t) > 0$, which tend to the origin as $t \to -\infty$. The corresponding solutions have the form

$$\begin{cases} x(t) = L \exp(2(t - t_1)) \\ y(t) = 2L \exp(2(t - t_1)) \end{cases} \quad L > 0, \, t_1 \in \mathbb{R}. \tag{22}$$

*Parameterizing the arc of circumference*. We solve the system (21) looking for solutions $(x(t), y(t))$ with $x(t) > 0$ and such that the trajectory passes through the point $Q$. The corresponding solutions have the form

$$\begin{cases} x(t) = 1 + r \sin(t - t_2) \\ y(t) = r \cos(t - t_2) \end{cases} \quad r > 0, \, t_2 \in \mathbb{R}. \tag{23}$$

Taking

$$r := \frac{2}{\sqrt{5}},$$

we have that the trajectory passes through the point $Q$ at the time

$$\hat{t} := \frac{\pi}{2} + t_2 \approx 2.677945045.$$

*The local stable manifold at the origin*. We solve the system (20), looking for solutions $(x(t), y(t))$ with $x(t) > 0$, $y(t) < 0$, which tend to the origin as $t \to +\infty$. The corresponding solutions have the form

$$\begin{cases} x(t) = L\exp(-2(t-t_3)) \\ y(t) = -2L\exp(-2(t-t_3)) \end{cases} \quad L > 0,\ t_3 \in \mathbb{R}. \tag{24}$$

We can take the same coefficient $L > 0$ in both (22) and (24), modifying (if necessary) $t_1$, $t_3$.

Now we are in position to fix the missing parameters $L > 0$ and $t_1 < t_2 < t_3$ in order to obtain the parametrization of the homoclinic solution.

We initiate conventionally assuming that at the time $t = 0$ the solution starts at the point

$$P_0 := \left(\frac{1}{5}, \frac{2}{5}\right),$$

which is the point of tangency of the local unstable manifold $y = 2x$ with the circumference $\mathcal{C}$. In this case, from equation (22), we obtain $t_1 = 0$ and

$$L := \frac{1}{5}.$$

Next, from equation (23) and having $r > 0$ already fixed as above, we determine the precise value of the time $t_2$ so that at the initial time $t = 0$, the solution of (23) starts at the point $P_0$. In this manner we obtain the system

$$\begin{cases} 1 + \dfrac{2}{\sqrt{5}}\sin(0-t_2) = \dfrac{1}{5} \\ \dfrac{2}{\sqrt{5}}\cos(0-t_2) = \dfrac{2}{5} \end{cases}$$

and hence

$$t_2 := \arcsin(2/\sqrt{5}).$$

As already observed the solution achieves its maximum in the $x$-component at the time

$$\hat{t} = \frac{\pi}{2} + \arcsin(2/\sqrt{5}).$$

Thus the analytic expression of the homoclinic solution $(x(t), y(t))$ is

$$x(t) := \begin{cases} \dfrac{1}{5}\exp(2t), & \text{for } t \le 0 \\ 1 + \dfrac{2}{\sqrt{5}}\sin(t - \arcsin(2/\sqrt{5})), & \text{for } 0 \le t \le \hat{t} \end{cases}$$

and

$$y(t) := \begin{cases} \dfrac{2}{5}\exp(2t), & \text{for } t \le 0 \\ \dfrac{2}{\sqrt{5}}\cos(t - \arcsin(2/\sqrt{5})), & \text{for } 0 \le t \le \hat{t}. \end{cases}$$

We do not need to study further the equations in order to glue the solutions of (23) with (24), because, by the symmetry of the system, we know that the homoclinic solution has symmetry with respect to $\hat{t}$, with $q_0(t)$ even and $v_0(t)$ odd with respect to the origin of the time-axis shifted at $\hat{t}$. Hence, the homoclinic solution, defined on the whole real line takes the form

$$x(t) := \begin{cases} \dfrac{1}{5}\exp(2t), & \text{for } t \le 0 \\ 1 + \dfrac{2}{\sqrt{5}}\sin(t - \arcsin(2/\sqrt{5})), & \text{for } 0 \le t \le 2\hat{t} \\ \dfrac{1}{5}\exp(-2(t - 2\hat{t})), & \text{for } t \ge 2\hat{t}. \end{cases} \tag{25}$$

and

$$y(t) = x'(t) := \begin{cases} \dfrac{2}{5}\exp(2t), & \text{for } t \le 0 \\ \dfrac{2}{\sqrt{5}}\cos(t - \arcsin(2/\sqrt{5})), & \text{for } 0 \le t \le 2\hat{t} \\ -\dfrac{2}{5}\exp(-2(t - 2\hat{t})), & \text{for } t \ge 2\hat{t} \end{cases} \tag{26}$$

*Introduction of the Melnikov function*. From equations (25) and (26), we have obtained the precise analytical expression of the homoclinic solution $\gamma_0(t) = (q_0(t), v_0(t))$, that we write as

$$q_0(t) := \begin{cases} \dfrac{1}{5}\exp(2(t + \hat{t})), & \text{for } t \le -\hat{t} \\ 1 + \dfrac{2}{\sqrt{5}}\cos(t), & \text{for } -\hat{t} \le t \le \hat{t} \\ \dfrac{1}{5}\exp(-2(t - \hat{t})), & \text{for } t \ge \hat{t}. \end{cases} \tag{27}$$

and

$$v_0(t) = q_{0'}(t) := \begin{cases} \dfrac{2}{5}\exp(2(t + \hat{t})), & \text{for } t \le -\hat{t} \\ -\dfrac{2}{\sqrt{5}}\sin(t), & \text{for } -\hat{t} \le t \le \hat{t} \\ -\dfrac{2}{5}\exp(-2(t - \hat{t})), & \text{for } t \ge \hat{t} \end{cases} \tag{28}$$

in order to make evident the symmetry with respect to $t = 0$ (see Figure 8).

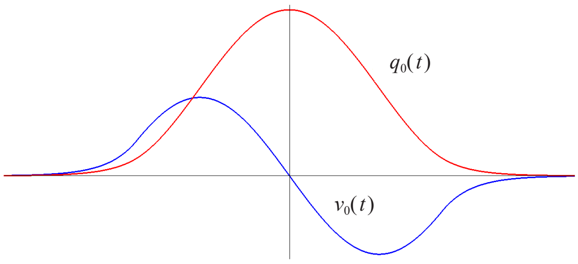


**Figure 8.** Graph associated with the function $v_0(t)$ and $q_0(t)$

We consider now the Melnikov function associated with equation

$$\ddot{x} + \varepsilon c\dot{x} + \psi(x) = \varepsilon p(\omega t), \tag{29}$$

which is defined as

$$M(\alpha) := \int_{-\infty}^{+\infty} \left( v_0(t) p(\omega(t+\alpha)) - c v_0(t)^2 \right) dt$$

$$= \int_{-\infty}^{+\infty} v_0(t) p(\omega(t+\alpha)) dt - c\int_{-\infty}^{+\infty} v_0(t)^2 \, dt. \tag{30}$$

We notice that the two integrals in $M(\alpha)$ are computable. Indeed, the function $v_0(t)$ has an explicit expression in (28) with exponential decay at $\pm\infty$ and therefore the integrals are convergent (for any periodic function $p(t)$). Moreover, the integrals can be easily computed, as we show with a concrete case, below.

To start with a simpler situation, we consider the case

$$p(t) = \sin(t).$$

Putting

$$p(\omega(t+\alpha)) = \sin(\omega t)\cos(\omega\alpha) + \cos(\omega t)\sin(\omega\alpha)$$

in (30) and using the fact that $v_0$ is odd, we have that $\int_{-\infty}^{+\infty} v_0(t)\cos(\omega t) dt = 0$ and hence

$$M(\alpha) = \cos(\omega\alpha)\int_{-\infty}^{\infty} v_0(t)\sin(\omega t) dt - c\int_{-\infty}^{\infty} v_0(t)^2 \, dt.$$

Next, using the fact that $v_0(t)\sin(\omega t)$ and $v_0(t)^2$ are even functions, we obtain

$$M(\alpha) = 2\cos(\omega\alpha)\int_{-\infty}^{0} v_0(t)\sin(\omega t) dt - 2c\int_{-\infty}^{0} v_0(t)^2 \, dt.$$

Hence, for any $\omega > 0$ such that the auxiliary function

$$N(\omega) := \int_{-\infty}^{0} v_0(t)\sin(\omega t)dt = \int_{0}^{+\infty} v_0(t)\sin(\omega t)dt \tag{31}$$

does not vanish, we can find a suitable $c$ (sufficiently small) such that $M(\alpha)$ has simple zeros located near the simples zeros of $\cos(\omega\alpha)$ and hence the Melnikov method applies.

In [27], the Authors prove the presence of chaotic dynamics for the case $\omega := \sqrt{2}$. With our method, computing $N(\sqrt{2}) \approxeq -4.508948445$, we obtain chaos according to Melnikov theorem [23, Theorem 1] for (29), provided that $|c|$ and $\varepsilon > 0$ are sufficiently small. Moreover, from the numerical study of the function $N(\omega)$, we can extend the result to all the values of $\omega$ such that $N(\omega) \neq 0$. A simple analysis of this function shows that the following result holds.

**Lemma 3.1** There exists $\omega^* \gtrapprox 2.367$ such that $N(\omega) < 0$ for each $0 < \omega < \omega^*$.

**Proof.** We observe that, for $N(\omega)$ defined as

$$N(\omega) = \int_{0}^{+\infty} v_0(t)\sin(\omega t)dt,$$

we have $N(\omega) \to 0$ for $\omega \to 0^+$ and

$$N'(\omega) = \int_{0}^{+\infty} t v_0(t)\cos(\omega t)dt$$

with

$$\lim_{\omega\to 0^+} N'(\omega) = \int_{0}^{+\infty} t v_0(t)dt \approxeq -8.870707261 < 0.$$

On the other hand, a direct calculation shows that $N(\pi) \approxeq 2.331126686 > 0$. This implies that there is a maximal interval $[0, \omega^*]$ such that $N(\omega) < 0$ for each $0 < \omega < \omega^*$. Using Maple software an approximate lower estimate for $\omega^*$ is given by $\omega^* \gtrapprox 2.367$. □

Figure 1 shows the behavior of $N(\omega)$ for ω in a right-neighborhood of the origin.

In any case, the analysis of the function shows that $N(\omega) \neq 0$ except for a discrete set of points.

## 4. Some numerical simulations

We conclude this paper, by showing some numerical simulations concerning the planar system

$$\begin{cases} \dot{x} = y \\ \dot{y} = -\psi(x) - \varepsilon p(\omega t) \end{cases} \tag{32}$$

with

$$\psi(x) = x - s(x)$$

defined as in (20).

Following [27], we choose to perform our examples in the special case

$$p(t) = \sin(t),$$

but similar portraits can be obtained for different forcing functions. Moreover, for this special choice of $p(t)$ we can take advantage of the function $N(\omega)$ defined in (31) for which we know that the Melnikov method applies for each frequency ω such that $N(\omega) \neq 0$.

In order to compare our results with [27] we do not consider any friction term of the form $\varepsilon c\dot{x}$, however, we point out that, as explained in the previous section, the Melnikov method works well also in the damped case for $c$ sufficiently small.

In [27] the authors proved the presence of chaotic dynamics for system

$$\begin{cases} \dot{x} = y \\ \dot{y} = -\psi(x) - \varepsilon \sin(\omega t) \end{cases} \tag{33}$$

for $\varepsilon = 1$ and $\omega = \sqrt{2}$. In our case, we find

$$N(\sqrt{2}) \approx -4.508948445,$$

hence our result applies providing an alternative way to prove chaos for the same equation considered in [27], at least for $\varepsilon > 0$ small.

As the next examples, we consider two choices of $\omega$, the first one in the interval $[0, \omega_1]$ and the second one in the interval $[\omega_1, \omega_2]$ , where $\omega_1$, $\omega_2$ are the first two zeros of $N(\omega)$. In both the examples we study the Poincaré map in the plane, by plotting the iterates of the map

$$\Phi_\varepsilon : z \mapsto \zeta(T; z),$$

where $\zeta(\cdot; z) = (x(\cdot), y(\cdot))$ is the solution of system (33) with initial point $\zeta(0; z) = z$ and

$$T = \frac{2\pi}{\omega}$$

is the fundamental period of the forcing term.

**Case 1** Let us consider

$$\omega = \frac{6}{5} = 1.2 < \omega_1.$$

In this case, $N(\omega) \approx -5.126375755 \neq 0$ and the Melnikov method can be applied.

Figure 9 below describes the iterates of the associated Poincaré map.

To stress the chaotic nature of certain solutions departing from some initial points, the next Figure 10 represents the x-component in dependence of the time variable $t$.

**Case 2** Let us consider

$$\omega = \frac{5}{2} = 2.5 \in [\omega_1, \omega_2].$$

In this case, $N(\omega) \approx 0.5594990220 \neq 0$ and the Melnikov method can be applied.

Figure 11 below describes the iterates of the associated Poincaré map.

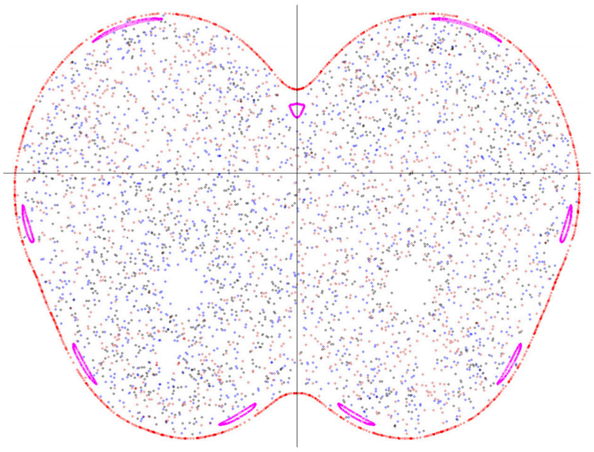

**Figure 9.** For the figure we have plotted the first 1,500 iterates of the Poincaré map $\Phi_\varepsilon$ for $\varepsilon = 0.3$ and $\omega = 6/5$, starting from the initial points $z_0 = (1, 0)$, $z_1 = (2, 0)$, $z_2 = (0, 0.4)$, $z_3 = (0, 0.6)$, $z_4 = (0, 0.3)$. The portrait makes clear the existence of a chaotic region surrounded by a presumably invariant curve, according to KAM theory (this is the Red line obtained from the initial point $z_3$), as well as the presence of isolas (in Magenta, obtained from the initial point $z_2$)

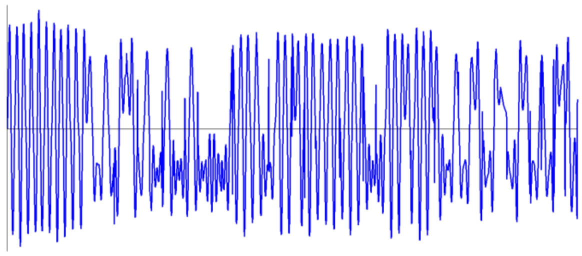

**Figure 10.** For the figure we have plotted the graph $(t, x(t))$ on the interval $[0, 733]$ where $(x(t), y(t))$ is the solution of (33) with $(x(0), y(0)) = z_4 = (0, 0.3)$. The parameters are $\varepsilon = 0.3$ and $\omega = 6/5$, are the same as for the study of the Poincaré map in Figure 9

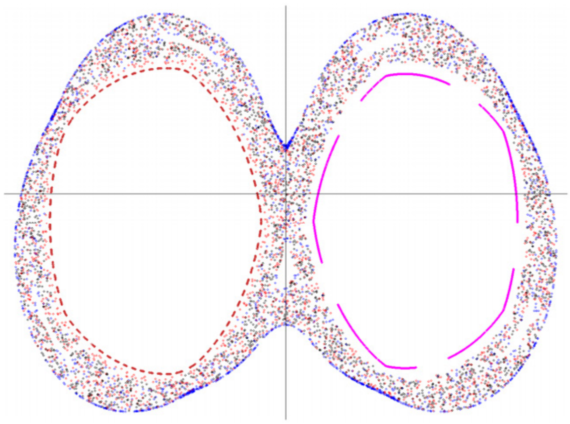

**Figure 11.** For the figure we have plotted the first 2,500 iterates of the Poincaré map $\Phi_\varepsilon$ for $\varepsilon = 0.3$ and $\omega = 5/2$, starting from the initial points $z_0 = (0, -0.1)$, $z_1 = (-0.4, 0.35)$, $z_2 = (0.4, 0.3)$, $z_3 = (1, 0.7)$, $z_4 = (0, 0.25)$. The portrait makes clear the presence of a chaotic regions bounded by presumably invariant curves, according to KAM theory (the Orange line obtained from the initial point $z_1$ and the Magenta obtained from the initial point point $z_2$ suggest the presence of quasiperiodic solutions or subharmonics of large order)

Figure 12 below stresses the chaotic nature of certain solutions of (33).

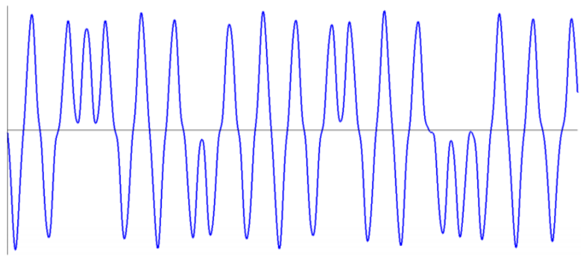

**Figure 12.** For the figure we have plotted the graph $(t, x(t))$ on the interval [1,800, 2,000] where $(x(t), y(t))$ is the solution of (33) with $(x(0), y(0)) = z_4 = (0, 0.25)$. The parameters are $\varepsilon = 0.3$ and $\omega = 5/2$, are the same as for the study of the Poincaré map in Figure 11

## 5. Conclusions

In this article we have proposed a new application of the Melnikov method for non-smooth vector fields to the periodically perturbed second order piecewise oscillator

$$\ddot{x} + \varepsilon c\dot{x} = \varepsilon p(\omega t) + s(x),$$

where $s(x)$ is a truncated signum function, namely it coincides with $x/|x|$ for $|x| \geq d > 0$ and is linear for $|x| \leq d$. The choice of this model has been motivated by a previous work by Pokrovskii, Rasskazov and Visetti [27] where the case $c = 0$, $\varepsilon = 1$, and $p(t) = \sin(t)$ was considered for the special value of $\omega = \sqrt{2}$.

Our main result in Section 3 and that in [27] are, in some sense, complementary: in [27] a weaker form of chaos is proved for a specific value of $\omega = \sqrt{2}$. In our case, we obtain a stronger form of chaos (Smale horseshoe) and a large interval of values for $\omega$. This greater generality is penalized by the fact that we need to consider small perturbations due to presence of an $\varepsilon$-coefficient in the forcing term. The need to consider a $\varepsilon$-perturbation is not due to our special case, but it is an intrinsic fact related to the Melnikov method and it appears as a common feature in all the corresponding applications (the search of the keyword "Melnikov method" produces more than 1,300 results on "MathSciNet"). In spite of the limitation of applicability of our result to small perturbations, we stress the fact that checking the existence of simple zeros for our Melnikov function $M(\alpha)$ introduced in (21) becomes a simple task once that a periodic perturbation $\varepsilon p(\omega t)$ is given. Indeed, we know explicitly the function $v_0(t)$ from (19) and from this fact, we can easily compute the corresponding function $M(\alpha)$. Thus, even if we have chosen $p(t) = \sin(t)$, in order to compare our result with that in [27], the possible range of applicability of our approach is truly wide, because we can repeat the same for other choices of $p(t)$ and values of $\omega$.

Finally, concerning the nature of chaotic dynamics which is obtained with our technique, we observe that, once we have shown that the Melnikov method is applicable to our model, then the result guarantees the conjugation of the associated Poincaré map with the Bernoulli shift automorphism, according to Smale [4] (which is the stronger form of chaos obtained in the literature). The piecewise nature of the nonlinearity does not change this fact, because we only need to have a well defined Poincaré map and this fact is ensured by the global Lipschitzianity of the restoring term in the Duffing equation.

## Conflict of interest

The authors declare no conflict of interest.

## References


[1] Mel'nikov VK. On the stability of a center for time-periodic perturbations. *Trudy Moskovskogo Matematicheskogo Obshchestva*. 1963; 12: 3-52.
[2] Guckenheimer J, Holmes P. Nonlinear oscillations, dynamical systems, and bifurcations of vector fields. *Journal of Applied Mechanics*. 1984; 51(4): 947.
[3] Smale S. Diffeomorphisms with many periodic points. In: *Differential and Combinatorial Topology (A Symposium in Honor of Marston Morse)*. N. J.: Princeton Univ. Press, Princeton; 1965. p. 63-80.
[4] Smale S. Differentiable dynamical systems. *Bulletin of the American Mathematical Society*. 1967; 73: 747-817.
[5] Moser J. Stable and random motions in dynamical systems. *Annals of Mathematics Studies, No. 77*. With special emphasis on celestial mechanics, Hermann Weyl Lectures, the Institute for Advanced Study, Princeton, N. J. N. J.: Princeton University Press, Princeton, Tokyo: University of Tokyo Press; 1973.
[6] Sovrano E, Zanolin F. The Ambrosetti-Prodi periodic problem: different routes to complex dynamics. *Dynamic Systems and Applications*. 2017; 26(3-4): 589-626.
[7] Battelli F, Palmer KJ. Chaos in the Duffing equation. *Journal of Differential Equations*. 1993; 101(2): 276-301.
[8] Kuznetsov YA. Elements of applied bifurcation theory. *Applied Mathematical Sciences*. 2nd ed. New York: Springer-Verlag; 1998.
[9] Den Hartog JP. *Mechanical Vibrations*. New York: Dover; 1985.
[10] Kunze M, Küpper T, You J. On the application of KAM theory to discontinuous dynamical systems. *Journal of Differential Equations*. 1997; 139(1): 1-21.
[11] Ortega R. Boundedness in a piecewise linear oscillator and a variant of the small twist theorem. *Proceedings of the London Mathematical Society*. 1999; 79(2): 381-413.
[12] Shaw SW, Holmes PJ. A periodically forced piecewise linear oscillator. *Journal of Sound and Vibration*. 1983; 90(1): 129-155.
[13] Battelli F, Fečkan M. On the chaotic behaviour of discontinuous systems. *Journal of Dynamics and Differential Equations*. 2011; 23(3): 495-540.
[14] Battelli F, Fečkan M. Nonsmooth homoclinic orbits, Melnikov functions and chaos in discontinuous systems. *Journal of Physics D: Applied Physics*. 2012; 241(22): 1962-1975.
[15] Battelli F, Fečkan M. General Melnikov approach to implicit ODE's. *Journal of Dynamics and Differential Equations*. 2022; 34(1): 365-397.
[16] Calamai A, Franca M. Mel'nikov methods and homoclinic orbits in discontinuous systems. *Journal of Dynamics and Differential Equations*. 2013; 25(3): 733-764.
[17] Chen X, Li T, Llibre J. Melnikov functions of arbitrary order for piecewise smooth differential systems in $\mathbb{R}^n$ and applications. *Journal of Differential Equations*. 2022; 314: 340-369.
[18] Fečkan M, Pospíšil M. *Poincaré-Andronov-Melnikov Analysis for Nonsmooth Systems*. Amsterdam: Elsevier/Academic Press; 2016.
[19] Franca M, Pospíšil M. New global bifurcation diagrams for piecewise smooth systems: transversality of homoclinic points does not imply chaos. *Journal of Differential Equations*. 2019; 266(2-3): 1429-1461.
[20] Kunze M. Non-smooth dynamical systems. *Lecture Notes in Mathematics*. Berlin: Springer-Verlag; 2000.
[21] Kukučka P. Melnikov method for discontinuous planar systems. *Nonlinear Analysis*. 2007; 66(12): 2698-2719.
[22] Li S, Zhang W, Hao Y. Melnikov-type method for a class of discontinuous planar systems and applications. *International Journal of Bifurcation and Chaos in Applied Sciences and Engineering*. 2014; 24(2):1450022.
[23] Li S, Gong X, Zhang W, Hao Y. The Melnikov method for detecting chaotic dynamics in a planar hybrid piecewise-smooth system with a switching manifold. *Nonlinear Dynamics*. 2017; 89(2): 939-953.
[24] Makarenkov O, Lamb JSW. Dynamics and bifurcations of nonsmooth systems: a survey. *Journal of Physics D: Applied Physics*. 2012; 241(22): 1826-1844.
[25] Si C, Tian R, Feng J, Yang X. Bifurcation and chaos for piecewise nonlinear roll system of rolling mill. *Advances in Mechanical Engineering*. 2017; 9(12): 1-8.
[26] Tian H, Han M. Limit cycle bifurcations of piecewise smooth nearHamiltonian systems with a switching curve. *Discrete and Continuous Dynamical Systems - B*. 2021; 26(10): 5581-5599.
[27] Pokrovskii A, Rasskazov O, Visetti D. Homoclinic trajectories and chaotic behaviour in a piecewise linear oscillator. *Discrete and Continuous Dynamical Systems - B*. 2007; 8(4): 943-970.
[28] Moon FC, Holmes PJ. A magnetoelastic strange attractor. *Journal of Sound and Vibration*. 1979; 65(2): 275-296.
[29] Holmes PJ, Moon FC. Strange attractors and chaos in nonlinear mechanics. *Journal of Applied Mechanics*. 1983;

50(4): 1021-1032.

[30] Zgliczyński P. Fixed point index for iterations of maps, topological horseshoe and chaos. *Topological Methods in Nonlinear Analysis*. 1996; 8(1): 169-177.

[31] Burns K, Weiss H. A geometric criterion for positive topological entropy. *Communications in Mathematical Physics.* 1995; 172(1): 95-118.

[32] Carbinatto MC, Kwapisz J, Mischaikow K. Horseshoes and the Conley index spectrum. *Ergodic Theory and Dynamical Systems*. 2000; 20(2): 365-377.

[33] Kennedy J, Yorke JA. Topological horseshoes. *Transactions of the American Mathematical Society*. 2001; 353(6): 2513-2530.

[34] Hale JK. *Ordinary Differential Equations*. 2nd ed. N. Y.: Robert E. Krieger Publishing Co., Inc., Huntington; 1980.

[35] Ding TR, Zanolin F. Subharmonic solutions of second order nonlinear equations: a time-map approach. *Nonlinear Analysis*. 1993; 20(5): 509-532.

[36] Boscaggin A, Fonda A, Garrione M. A multiplicity result for periodic solutions of second order differential equations with a singularity. *Nonlinear Analysis*. 2012; 75(12): 4457-4470.

[37] Fonda A, Manásevich R, Zanolin F. Subharmonic solutions for some second-order differential equations with singularities. *SIAM Journal on Mathematical Analysis*. 1993; 24(5): 1294-1311.

[38] Palmer KJ. Transversal heteroclinic points and Cherry's example of a nonintegrable Hamiltonian system. *Journal of Differential Equations*. 1986; 65(3): 321-360.

[39] Holmes P. A nonlinear oscillator with a strange attractor. *Philosophical Transactions of the Royal Society A*. 1979; 292(1394): 419-448.